Journal of Environmental Science and Engineering B 4 (2015) 1-8
doi: 10.17265/2162-5263/2015.01.001

Precise Control in Characteristics of Nano-particulate MFI-Type Ferrisilicate and Their Catalysis in the Conversion of Dimethyl Ether into Light Olefins

Hiroki Kobayashi[1], Masafumi Nakaya[2], Kiyoshi Kanie[2] and Atsushi Muramatsu[2]

1. School of Engineering, Tohoku University, Sendai 980-8579, Japan

2. Institute of Multidisciplinary Research for Advanced Materials, Tohoku University, Sendai 980-8577, Japan

Abstract: This study reports the synthesis of size-controlled Fe-MFI (Fe-substituted zeolites with the MFI topology) and their catalytic performances for DTO (dimethyl ether-to-olefins) reaction. The amount of HCl and aging temperature were decisive factors to control the particle size of Fe-MFI in the range of 50 nm to 600 nm. The introduction of Fe^{3+} ions into the zeolitic framework was confirmed by UV (ultraviolet)-visible spectroscopy. In addition, it was observed that the strength of acid site in prepared Fe-MFI was weaker than that of commercial ZSM-5. With decrease in the particle size, the amount of deposited coke decreased so that the catalyst life for the DTO reaction was well promoted. The present catalysts showed the higher light-olefin selectivity ($C_2^=$ + $C_3^=$ + $C_4^=$) than commercial ZSM-5 catalysts mainly due to the suppression of the formation of paraffins; however, the Fe-MFI catalysts were deactivated rapidly because of their low activity for the cracking of alkenes.

Key words: Nanosized Fe-MFI, ZSM-5, dimethyl ether-to-olefin reaction, light-olefin selectivity.

1. Introduction

Light olefins are important raw materials for the production of diverse petrochemicals so that their demands are expected to increase in the future. In recent years, the production of olefins from methanol (MTO: methanol-to-olefins) or DME (dimethyl ether) (DTO: DME-to-olefins) has been focused attention to efficiently use the non-oil resources as the feedstocks of olefins [1, 2]. The MTO/DTO reactions are promoted by solid acids; in particular, microporous zeolites are well known as the catalysts for such reactions. Although zeolites with narrow pores (e.g., chabazite) exhibit high light-olefin selectivity in these reactions, their activities are rapidly deactivated because of the deposition of coke. Therefore, a fluidized bed reactor is mainly used for these zeolites because of the frequent removal of carbonaceous residues. On the other hand, zeolites with medium pores, e.g., MFI-type zeolite (ZSM-5), exhibits poor selectivity for light olefins, even though the amount of coke deposited is less than that by narrow-porous zeolites. Although ZSM-5 catalysts are attractive for fixed-bed processes with a long operating time without regeneration treatments, a further increase in the light-olefin selectivity and lifetime of catalysts are desired for such medium-pore zeolites.

First, the undesired reactions such as hydride transfer or cyclization to fabricate paraffins and aromatics as a by-product should be suppressed so that the selectivity of light olefins in MTO or DTO reaction may be promoted. Since ZSM-5 well catalyzes hydride transfer or cyclization reactions, its pore size or acidity are needed to promote in order to control its reactivity of the present reaction. The substitution of Al in the zeolitic framework with the other transition element can control their acidic properties. MFI-type metallosilicates containing trivalent cations (e.g., B^{3+}, Fe^{3+} and Ga^{3+}) show weaker acidic sites than ZSM-5 [3, 4]. As Inui [5] and

Corresponding author: Masafumi Nakaya, Ph.D., research field: nano-materials. E-mail: m-nakaya@tagen.tohoku.ac.jp.

Inui et al. [6] have investigated, the catalytic activities of a series of MFI-type metallosilicates for the MTO reaction, and Fe-, Pt-, and Co-silicates have showed higher light-olefin selectivity than other metallosilicates. In particular, Fe-silicates showed the lowest selectivity to aromatics so that methanol conversion into light olefins was promoted efficiently.

Second, the diffusion of reactants into micropores and/or products from them should be enhanced so as to prolong the lifetime of catalysts. The reduction in particle size of zeolites may result in the decrease in diffusion path length [7]. In the other attempt, mesopores have been introduced into zeolites so as to improve diffusion properties [8, 9]. As a result, their lifetime of ZSM-5 has been reported to promote considerably for the MTO reaction [10, 11]. However, light-olefin selectivity decreased due to an increase in the active sites on the surface of particles or mesopores. Both these approaches have been also applied to the enhancement in the catalytic performances of metallosilicates [12].

In this study, Fe-MFI (Fe-substituted MFI zeolites) with size precisely controlled have been prepared by hydrothermal method to investigate the effect of diffusion properties on the light-olefin selectivity, catalyst lifetime, and the amount of coke deposited in the reaction of undiluted, or neat, dimethyl ether. The effects of the acid strength of the catalysts on their catalytic properties were also evaluated by comparing the Fe-MFI catalyst with a commercially available ZSM-5 catalyst.

2. Experiments

The size-controlled Fe-MFI was hydrothermally synthesized with different amounts of aqueous HCl in the precursor solution and preheating time. The established synthesis conditions for the Fe-MFI (labeled F1-F4) are shown in Table 1. The reaction conditions for F1 were used first, and they were modified by preheating treatments (F2 and F4) and/or the addition of aqueous HCl in the precursor solution (F3 and F4). The details of the synthesis are as follows: the aqueous solutions of $Fe(NO_3)_3$ (Wako Pure Chemical Industries Ltd.), tetrapropylammonium hydroxide (TPAOH, Tokyo Chemical Industry Co., Ltd.), and HCl (Wako Pure Chemical Industries Ltd.) were mixed. After stirring the resulting solution for 10 min, tetraethyl orthosilicate (TEOS, Wako Pure Chemical Industries Ltd.) was added. The molar composition of the mixture was as follows: 17 mmol TEOS, 0.34 mmol $Fe(NO_3)_3$, 8.5 mmol TPAOH, 510 mmol H_2O, and 0 mmol or 1.7 mmol HCl. The solution was stirred for 6 h at 0 °C and then stirred for 42 h at room temperature. The solution was added to a Teflon-lined stainless-steel autoclave and preheated at 70 °C for 0 h or 24 h and then heated at 160 °C for 48 h under vertical rotation (10 rpm). The product was centrifugally washed 5 times with deionized water and dried at 60 °C. The organic template was removed by calcination at 540 °C for 12 h in air. The resulting powder was ion exchanged by adding aqueous NH_4Cl and calcined again at 540 °C to form Brønsted acid sites.

The product phase was identified by powder XRD (X-ray diffraction) analysis (Rigaku Ultima IV) using Cu Kα radiation from 40 kV to 40 mA. The crystal morphology and size of the resulting samples were identified by FE-SEM (field emission-scanning electron microscope) (Hitachi High-Tech S-4800) after coating the sample with gold. The average

Table 1 Synthesis conditions of Fe-MFI.

Sample	Preheating time at 70 °C (h)	Heating time at 160 °C (h)	Molar ratios in precursor solutions (mol·mol^{-1})			
			HCl/Si	Si/Fe	H_2O/Si	TPA/Si
F1	0	48	0	50	30	0.5
F2	24	48	0	50	30	0.5
F3	0	48	0.1	50	30	0.5
F4	24	48	0.1	50	30	0.5

particle size was obtained by measuring the diameters of 200 particles on the FE-SEM images. The chemical composition of the samples was determined by XRF (X-ray fluorescence) analysis (Rigaku ZSX Primus II). The surface area and pore volume of the samples were determined by N_2 adsorption at 77 K (BEL Japan, Inc. BELSORP mini). All the samples were preheated at 400 °C for 2 h in N_2 atmosphere prior to the measurements. The external surface areas were calculated by the *t*-plot method. The coordination state of Fe^{3+} species was characterized by diffuse reflectance UV (ultraviolet)-visible absorption using a U-3900 spectrometer (Hitachi High-Tech). The obtained reflectance spectra were converted into absorption using Kubelka-Munk function.

The acid site density and strength of Fe-MFI and ZSM-5 catalysts were evaluated by the TPD (temperature-programmed desorption) of ammonia using an instrument equipped with quadrupole mass spectrometer (BEL Japan, Inc., BELCAT). NH_3 (5% in He, 60 mL·min^{-1}) was adsorbed on the samples at 100 °C for 30 min after treating with He (500 °C, 1 h, 60 mL·min^{-1}). After the saturation of NH_3 adsorption, the sample was exposed to water vapors (100 °C, 4 kPa, 30 min) twice to remove the weakly held NH_3 species, such as hydrogen-bonded NH_3. The sample cell was heated from 100 °C to 700 °C at a rate of 10 °C·min^{-1}, and the desorbed NH_3 was measured by the amount of fragment of m/z = 16 in the quadrupole mass spectra.

The nature of OH groups was measured by DRIFTS (diffuse reflectance infrared spectroscopy) using an instrument equipped with an environmental chamber (FTS7000, Digilab). Prior to the experiments, the samples were preheated at 450 °C for 1 h in Ar. The DRIFTS spectra were recorded after cooling at 2 cm^{-1} resolution. All the spectra were normalized at the intensity of skeletal band at 2,000 cm^{-1}.

The DTO reaction over the catalysts was carried out in a fixed-bed quartz reactor at atmospheric pressure. The sample powder was pressed at 19.6 kN for 30 min, crushed, and sieved in the range 32-44 mesh. A mixture of 0.20 g of the sample and 0.84 g of quartz sand (20-28 mesh) was placed in the reactor and preheated at 550 °C in Ar for 1 h. After the preheating, neat DME was fed over the catalyst at 450 °C with 5.8 g·h·mol^{-1} in *W*/*F* (mass of the catalyst (g) divided by the feed rate of DME (mol·h^{-1})). The product was cooled to 120 °C, and C_2 to C_4 olefins were detected using an on-line gas chromatograph equipped with a flame ionization detector (Ar carrier, Shimadzu 8A; Gaskuropack 54 column). The amounts of coke deposited on the catalysts were measured by TG (thermogravimetric) analyses (SII TG/DTA 7200). The coke amount was defined as the weight difference between 300 °C and 800 °C.

3. Results and Discussion

The FE-SEM and TEM (transmission electron microscopy) images of the as-prepared Fe-MFI catalysts are shown in Fig. 1 and the XRD patterns are shown in Fig. 2. All the Fe-MFI catalysts were identified as a pure MFI-type structure and shaped as spherical with rugged surfaces. The particle sizes of the Fe-MFI catalysts were varied from 50 nm to 600 nm with change in HCl concentration and preheating temperature. The minimum size, 50 nm, for Fe-MFI nanoparticles was successfully controlled in the case of F4. The preheating treatment may make nucleation promote so that the number of crystal nuclei is increased because the particle size was decreased with the increase in preheating time (Fig. 3). Moreover, a low preheating temperature hinders the growth of crystal nuclei [13]. Therefore, the introduction of low-temperature ageing increased the number of nuclei. On the other hand, the increase in HCl concentration may result in rise of nuclei number, since the higher pH generally promotes the nucleation for oxides particles [14] as well as it enhances the transformation of random T-O-T networks (T: Si, Al, Fe, etc.) into a regular crystal structure [15] (Fig. 4).

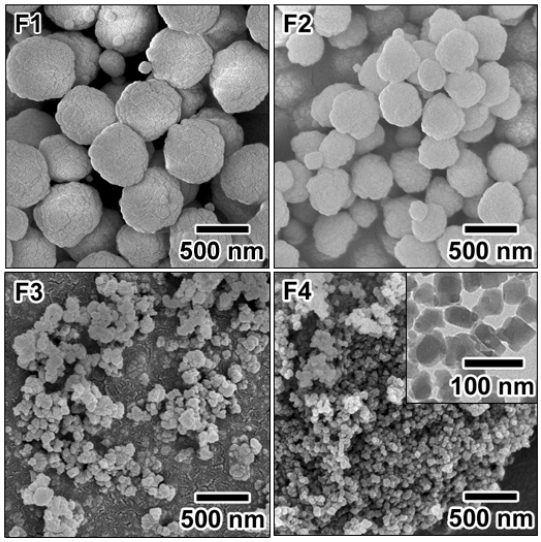

Fig. 1 SEM images of the resulting Fe-MFI catalyst under the synthesis conditions for F1-F4 shown in Table 1. Inset image: TEM image of F4.

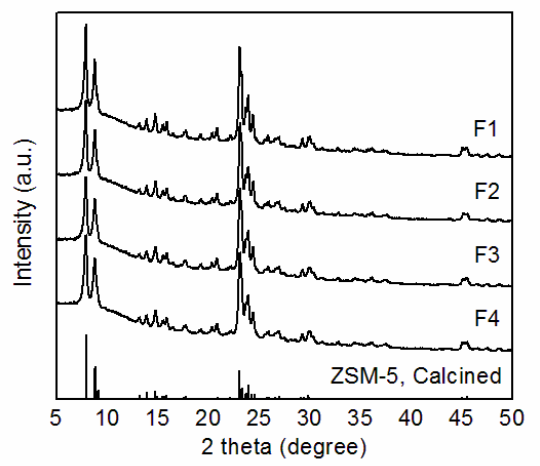

Fig. 2 XRD patterns of as-synthesized Fe-MFI catalyst under the synthesis conditions for F1-F4 shown in Table 1.

However, the number of nuclei reduced at an extremely high pH level because of the increase in the solubility of zeolites [16, 17] so that it reaches the maximum value at a medium pH (HCl/Si = 0.1), that is, the particle size reaches the minimum. This result is consistent with the relationship between the particle size and pH in the synthesis of Silicalite-1 reported previously [18, 19].

The detailed properties of the Fe-MFI catalysts, F1 and F4, are evaluated so that the effects of the particle size will be clarified on the catalytic activity for the DTO reaction. Moreover, their comparison

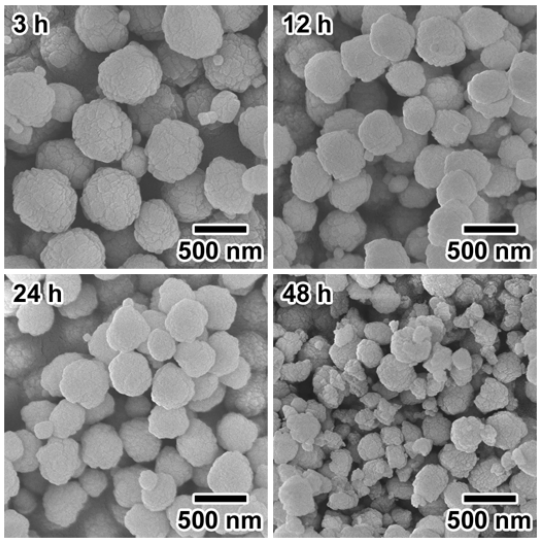

Fig. 3 SEM images of the resulting Fe-MFI with different preheating time (preheating temperature: 70 °C, the other synthesis conditions were the same as F1).

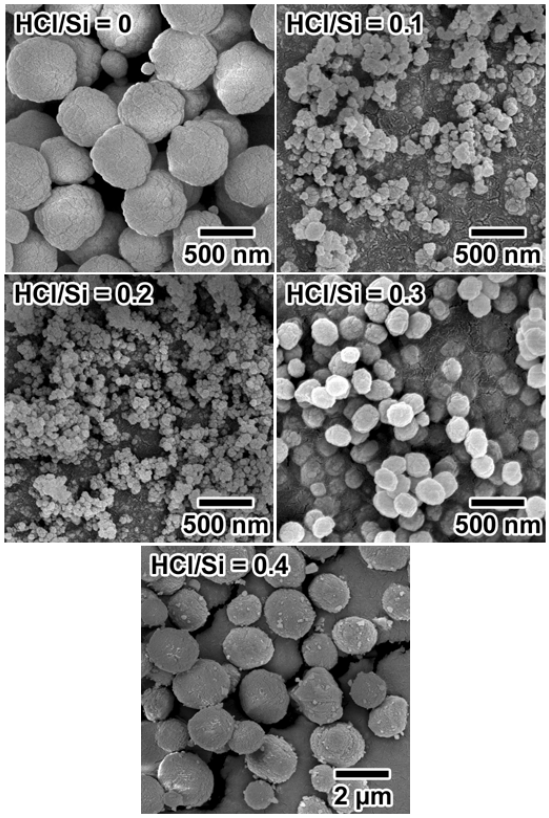

Fig. 4 SEM images of the resulting Fe-MFI with different amount of HCl (preheating time: 0 h).

with ZSM-5 (labeled CZ) one prepared by heating NH_4-formed ZSM-5 was also evaluated as an effect of the difference between the framework cations. The physicochemical properties of those samples are

Table 2 Physicochemical properties of the catalysts.

Catalyst	Particle size (nm)	S_{BET} ($m^2 \cdot g^{-1}$)	External surface area ($m^2 \cdot g^{-1}$)	Al or Fe content ($mmol \cdot g^{-1}$)	NH_3 capacity ($mmol \cdot g^{-1}$)	ΔH_{NH3} ($kJ \cdot mol^{-1}$)
F1	600	493	21	0.37	0.33	124
F4	50	491	87	0.33	0.33	123
CZ	200-1,500	474	46	0.38	0.40	131

summarized in Table 2. The particle sizes were 600 nm (F1), 50 nm (F4), and 200-1,500 nm (CZ). The results of N_2 adsorption and desorption isotherms identified these samples as type I so that they were microporous materials. Three samples had almost the same BET (Brunauer-Emmett-Teller) surface areas. However, F4 showed a much higher external surface area than the other samples because of finer particle size.

The UV-visible spectra of F1 and F4 catalysts are shown in Fig. 5. The main absorption peaks were observed around 215, 240 and 280 nm. The absorption peaks at 215 nm and 240 nm indicate the existence of isolated Fe^{3+} ions in tetrahedral coordination (≈ framework Fe^{3+}), and the absorption peak at 280 nm indicates the existence of isolated Fe^{3+} ions in octahedral coordination [20]. Moreover, Fe^{3+} species in small clusters or Fe_2O_3 nanoparticles may not be contaminated in F1 and F4 catalysts because the absorption above 300 nm was insignificant. Therefore, Fe^{3+} ions were well replaced with those in the T site in the zeolite framework, even though a part of Fe^{3+} ions was octahedrally coordinated, which may be formed by the interactions between the framework Fe^{3+} ions and neighboring Si-OH groups. They must be formed by the hydrolysis of framework Si-O-Si bonds in the first calcination process. This is supported by the fact that the band ~280 nm in F1 and F4 catalysts was not observed before the first calcination process (broken line in Fig. 5), in which the micropores were filled with organic templates.

Fig. 6 shows the NH_3-TPD spectra of these three samples. The peak around 300 °C to 400 °C can be attributed to the desorption of NH_3 from the samples. Table 2 shows the desorbed amount of ammonia calculated from the peak areas and the amount of trivalent cations measured by XRF. The ammonia

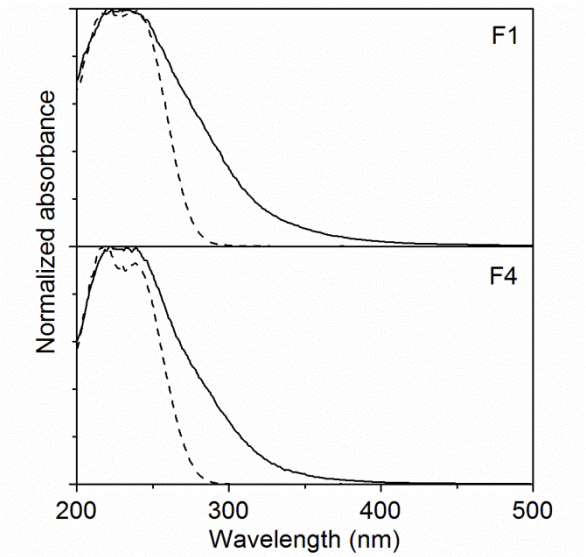

Fig. 5 UV-visible spectra of the resulting Fe-MFI catalysts prepared under the reaction conditions for F1 and F4 catalysts shown in Table 1.

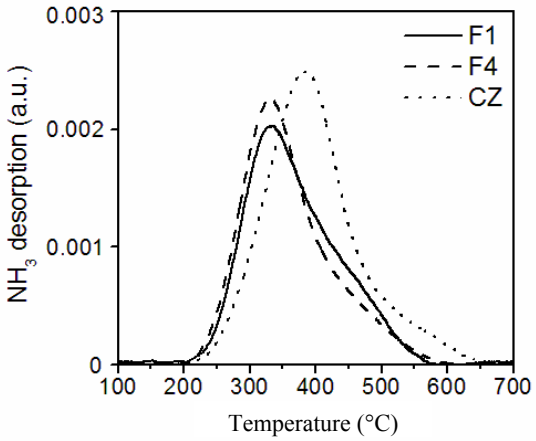

Fig. 6 TPD spectra of the obtained Fe-MFI catalysts prepared under the reaction conditions for F1 and F4 catalysts shown in Table 1 and the obtained ZSM-5 (CZ) as the standard.

desorption amount was roughly consistent with the content of Fe or Al. Therefore, almost all the acid sites were generated by the introduction of Fe^{3+} or Al^{3+} ions. Table 2 also shows the desorption heat of ammonia from the samples (ΔH_{NH3}) by the method

proposed by Niwa et al. [21]. Since the ΔH_{NH3} of CZ was higher than those of F1 or F4, the acid strength of Fe-MFI was lower than that of ZSM-5. The acid site strengths of F1 and F4 catalysts were almost the same so that the particle size was insignificant in affecting the acid site strength of the Fe-MFI catalyst.

Fig. 7 shows the DRIFTS spectra of these three samples in the OH stretching region. First, the absorption band at 3,630 cm^{-1} (F1 and F4 catalysts) or 3,610 cm^{-1} (CZ) is attributed to the bridging hydroxyls observed in every sample. These peaks support the presence of acid sites originated from the "Si (OH) Fe" structure. All the samples also possessed the silanol groups due to the presence of the absorption peaks at 3,700-3,750 cm^{-1}. The absorption in this region consisted of an isolated silanol bond (≡Si-OH) at the surface (at 3,745 cm^{-1}) and inside micropores (at 3,726 cm^{-1} or 3,700 cm^{-1}) [22]. The peak for the isolated silanol group in F4 catalyst red-shifted compared to the other samples, indicating the presence of large amounts of isolated silanol groups on the surface of F4.

Fig. 8 shows the product selectivity obtained for the fresh catalysts (5 min on stream). F1 and F4 catalysts showed higher light-olefin selectivity ($C_2^= + C_3^= + C_4^=$) and lower light-paraffin one ($C_2 + C_3 + C_4$) than those of CZ. The hydride transfer reaction may be suppressed by decrease in the reactivity of carbocations because the olefin-to-paraffin ratio of the Fe-MFI catalyst was higher than that of the ZSM-5 catalyst. As F1 and F4 catalysts also showed higher selectivity to methane than CZ, the Fe-MFI catalysts have higher catalytic activity for the dehydrogenation reaction than ZSM-5.

The effect of the particle size of the Fe-MFI catalyst on the product selectivity was negligible in contrast to that of ZSM-5 [10], possibly because of the decrease in the acidic strength of Fe-MFI.

The changes in the conversion of DME over these three catalysts with time on stream are compared in Fig. 9. Methanol was regarded as 1/2 of the molecule

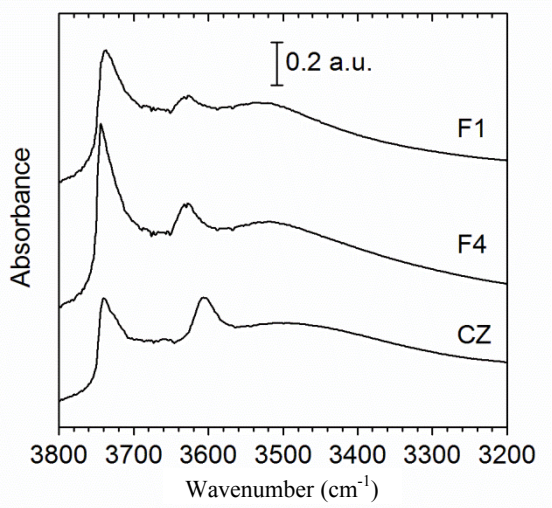

Fig. 7 DRIFTS spectra for the OH stretching region of the obtained Fe-MFI catalysts prepared under the reaction conditions for F1 and F4 catalysts shown in Table 1 and the obtained ZSM-5 (CZ) as the standard.

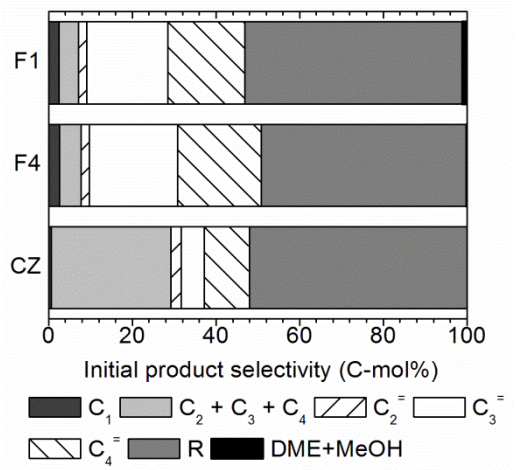

Fig. 8 Product selectivity obtained over the freshly prepared Fe-MFI catalysts prepared under the reaction conditions for F1 and F4 catalysts shown in Table 1 and the obtained ZSM-5 (CZ) as the standard.

of unreacted DME. The time when the conversion of DME decreased to 50% was defined as the catalyst lifetime (Table 3), based on the model proposed by Janssens [23]. F4 catalyst showed a longer catalyst lifetime for the DTO reaction than F1 catalyst. CZ showed the longest lifetime among the three samples. Table 3 also shows the amounts of carbonaceous residues deposited on the catalysts after 1 h or 4 h on stream. The coke amount of F4 catalyst was less than that of F1 catalyst but almost the same as that of CZ.

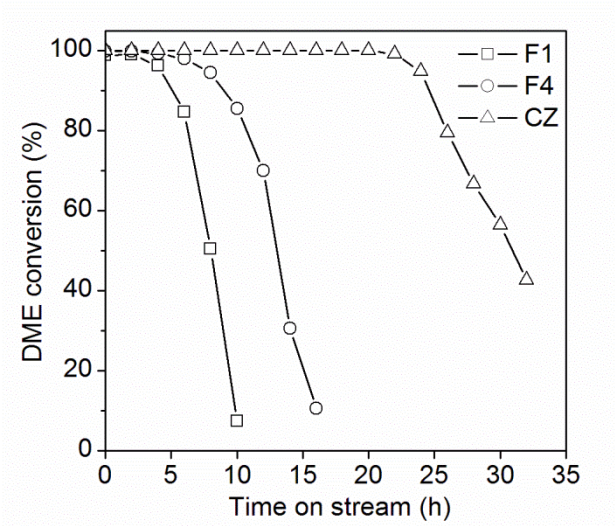

Fig. 9 Conversion of DME over the obtained Fe-MFI catalysts prepared under the reaction conditions for F1 and F4 catalysts shown in Table 1 and the obtained ZSM-5 (CZ) as the standard.

Table 3 Catalyst lifetime and amount of coke.

Catalyst	Catalyst lifetime (h)	Amount of coke (wt%)	
		1 h	4 h
F1	8	4.5	11
F4	13	2.7	6.3
CZ	31	3.1	5.9

The suppression of coke formation due to the decrease in the particle size results in the promotion of the catalyst lifetime of F4 because the miniaturization of the size of the catalyst facilitated the diffusion of products to the outside of the micropores. The CZ size was larger than F4, but the coke amount was almost the same, since the coke-deposition rate on ZSM-5 may be slower than that of Fe-MFI. Namely, the low activity of the Fe-MFI catalyst in the cracking reaction of higher (C_5^+) olefins was reported owing to its weak acidity [24].

4. Conclusions

Fe-MFI catalysts in the size range 50-600 nm were successfully synthesized through the control of the reaction conditions under the conventional hydrothermal method. The pH with aqueous HCl and the preheating treatment at 70 °C resulted in effective decrease in the particle size. The obtained Fe-MFI catalysts showed weaker acidic sites (ΔH_{NH3} = 122-124 kJ·mol^{-1}) than that of commercially available ZSM-5 (ΔH_{NH3} = 131 kJ·mol^{-1}) and exhibited the higher light-olefin selectivity ($C_2^=$ ~ $C_4^=$, Al: 19%, Fe: 40%) by the suppression to the hydride transfer reaction. The size effect of Fe-MFI catalyst on the catalyst lifetime was very effective, because the amount of deposited coke significantly was reduced by decrease in the particle size. However, the Fe-MFI catalysts showed a short catalyst lifetime compared to ZSM-5 owing to their lower cracking activity for heavy alkenes. The catalyst lifetime of Fe-MFI catalysts can be improved by the addition of other strong acidic sites.

References

[1] Stöcker, M. 1999. "Methanol-to-Hydrocarbons: Catalytic Materials and Their Behavior." *Microporous and Mesoporous Materials* 29: 3-48.

[2] Olsbye, U., Svelle, S., Bjørgen, M., Beato, P., Janssens, T. V. W., Joensen, F., Bordiga, S., and Lillerud, K. P. 2012. "Conversion of Methanol to Hydrocarbons: How Zeolite Cavity and Pore Size Controls Product Selectivity." *Angewandte Chemie International Edition* 51: 5810-31.

[3] Chu, C. T.-W., and Chang, C. D. 1985. "Isomorphous Substitution in Zeolite Frameworks. 1. Acidity of Surface Hydroxyls in [B]-, [Fe]-, [Ga]-, and [Al]-ZSM-5." *The Journal of Physical Chemistry* 89: 1569-71.

[4] Datka, J., and Abramowicz, T. 1994. "Hydroxy Groups in Ferrisilicates Studied by IR Spectroscopy." *Journal of Chemical Society, Faraday Transactions* 90: 2417-21.

[5] Inui, T. 1985. "Hydrocarbon Synthesis from Syngas on Composite Catalysts of Metal Oxide and Shape-Selective Zeolites." *Sekiyu Gakkaishi* 28: 279-92.

[6] Inui, T., Matsuda, H., Yamase, O., Nagata, H., Fukuda, K., Ukawa, T., and Miyamoto, A. 1986. "Highly Selective Synthesis of Light Olefins from Methanol on a Novel Fe-Silicate." *Journal of Catalysis* 98: 491-501.

[7] Tosheva, L., and Valtchev, V. P. 2005. "Nanozeolites: Synthesis, Crystallization Mechanism, and Applications." *Chemistry of Materials* 17: 2494-513.

[8] Ogura, M., Shinomiya, S., Tateno, J., Nara, Y., Nomura, M., Kikuchi, E., and Matsukata, M. 2001. "Alkali-Treatment Technique—New Method for Modification of Structural and Acid-Catalytic Properties of ZSM-5 Zeolites." *Applied Catalysis A: General* 219: 33-43.

[9] Groen, J. C., Zhu, W., Brouwer, S., Huynink, S. J., Kapteijn,

F., Moulijn, J. A., and Peŕez-Ramírez, J. 2007. "Direct Demonstration of Enhanced Diffusion in Mesoporous ZSM-5 Zeolite Obtained via Controlled Desilication." *Journal of the American Chemical Society* 129: 355-60.

[10] Sugimoto, M., Katsuno, H., Takatsu, K., and Kawata, N. 1987. "Correlation between the Crystal Size and Catalytic Properties of ZSM-5 Zeolites." *Zeolites* 7: 503-7.

[11] Bjørgen, M., Joensen, F., Holm, M. S., Olsbye, U., Lillerud, K. P., and Svelle, S. 2008. "Methanol to Gasoline over Zeolite H-ZSM-5: Improved Catalyst Performance by Treatment with NaOH." *Applied Catalysis A: General* 345: 43-50.

[12] Mentzel, U. V., Højholt, K. T., Holm, M. S., Fehrmanna, R., and Beato, P. 2012. "Conversion of Methanol to Hydrocarbons over Conventional and Mesoporous H-ZSM-5 and H-Ga-MFI: Major Differences in Deactivation Behavior." *Applied Catalysis A: General* 417: 290-7.

[13] Guth, J. L., and Kessler, H. 1999. "Synthesis of Aluminosilicate Zeolites and Related Silica-Based Materials." In *Catalysis and Zeolites,* edited by Weitkamp, J., and Puppe, L. Berlin: Springer.

[14] Sugimoto, T. 2001. *Monodispersed Particles.* Amsterdam: Elsevier.

[15] Cundy, C. S., and Cox, P. A. 2005. "The Hydrothermal Synthesis of Zeolites: Precursors, Intermediates and Reaction Mechanism." *Microporous and Mesoporous Materials* 82: 1-78.

[16] Persson, A. E., Schoeman, B. J., Sterte, J., and Otterstedt, J. E. 1995. "Synthesis of Stable Suspensions of Discrete Colloidal Zeolite (Na, TPA) ZSM-5 Crystals." *Zeolites* 15: 611-9.

[17] Barrer, R. M. 1981. "Zeolites and Their Synthesis." *Zeolites* 1: 130-40.

[18] Fegan, S. G., and Lowe, B. M. 1986. "Effect of Alkalinity on the Crystallization of Silicalite-1 Precursors." *Journal of the Chemical Society, Faraday Transactions 1: Physical Chemistry in Condensed Phases* 82: 785-99.

[19] Yang, S., Navrotsky, A., Wesolowski, D. J., and Pople, J. A. 2004. "Study on Synthesis of TPA-Silicalite-1 from Initially Clear Solutions of Various Base Concentrations by in Situ Calorimetry, Potentiometry, and SAXS." *Chemistry of Materials* 16: 210-9.

[20] Bordiga, S., Buzzoni, R., Geobaldo, F., Lamberti, C., Giamello, E., Zecchina, A., Leofanti, G., Petrini, G., Tozzola, G., and Vlaic, G. 1996. "Structure and Reactivity of Framework and Extraframework Iron in Fe-Silicalite as Investigated by Spectroscopic and Physicochemical Methods." *Journal of Catalysis* 158: 486-501.

[21] Niwa, M., Katada, N., Sawa, M., and Murakami, Y. 1995. "Temperature-Programmed Desorption of Ammonia with Readsorption Based on the Derived Theoretical Equation." *The Journal of Physical Chemistry* 99: 8812-6.

[22] Barbera, K., Bonino, F., Bordiga, S., Janssens, T. V. W., and Beato, P. 2011. "Structure-Deactivation Relationship for ZSM-5 Catalysts Governed by Framework Defects." *Journal of Catalysis* 280: 196-205.

[23] Janssens, T. V. W. 2009. "A New Approach to the Modeling of Deactivation in the Conversion of Methanol on Zeolite Catalysts." *Journal of Catalysis* 264: 130-7.

[24] Bortnovsky, O., Sazama, P., and Wichterlova, B. "Cracking of Pentenes to C_2-C_4 Light Olefins over Zeolites and Zeotypes Role of Topology and Acid Site Strength and Concentration." *Applied Catalysis A: General* 287: 203-13.